Cytochrome *c* Peroxidase Complexed with Cytochrome *c* Has an Unperturbed Heme Moiety†

Jianling Wang,*,‡ Randy W. Larsen,§ Susan J. Moench,|| James D. Satterlee,⊥ Denis L. Rousseau,‡ and Mark R. Ondrias*,#

Department of Chemistry, University of New Mexico, Albuquerque, New Mexico 87131, Department of Chemistry, Washington State University, Pullman, Washington 99164, Department of Chemistry, University of Hawaii, Honolulu, Hawaii 19822, and AT&T Bell Laboratories, Murray Hill, New Jersey 07974

Received August 9, 1995; Revised Manuscript Received November 2, 1995⊗

ABSTRACT: Transient resonance Raman, Raman difference, circular dichroism (CD), and optical absorption studies have been carried out on the electrostatic complexes formed by yeast cytochrome *c* peroxidase (CCP) with horse cytochrome *c* (Cytc) in low ionic strength solutions. In all the complexes examined [e.g., CCP(II)/Cytc(II), CCP(III)/Cytc(II), CCP(III)/Cytc(III)], the local heme environments of both proteins are largely unperturbed upon complexation. Specifically, CCP preserves a completely pentacoordinate high-spin heme in both its ferric and ferrous forms in CCP/Cytc complexes and uncomplexed mixtures. We found no evidence corroborating the previously reported increase in the low-spin fraction of CCP heme upon complexation with Cytc [Hildebrandt et al. (1992) *Biochemistry 31,* 2384−2392]. Instead, our Raman data strongly suggest that the H-bonding networks in the distal and proximal pockets of CCP are well maintained in the complexes. On the other hand, CD spectra of CCP(III)/Cytc(III) complexes showed substantial variations (relative to the uncomplexed mixtures) in the far-UV region, reflecting some protein conformational rearrangements. In addition, the spectral data suggest that complexation with Cytc affects the previously observed pH-dependent flexibility of the heme structure of CCP and thus influences the photodynamics of the CCP active site.

Cytochrome *c* peroxidase (CCP)[1] is a relatively small catalytic heme protein (Poulos & Finzel, 1984; Mauro et al., 1989; Anni & Yonetani, 1992) that spontaneously forms noncovalent (electrostatic) complexes with various cytochromes *c* (Cytc) in low ionic strength solutions near neutral pH (Cokic & Erman, 1987; Satterlee et al., 1987). We have carried out Raman, CD, and optical studies of the electrostatic 1:1 complexes of these two proteins. Whereas both 1:1 and 1:2 (CcP:cytc) complexes have been shown to be capable of intramolecular electron transfer (Hazzard et al., 1987; Hahm et al., 1992; Zhou & Hoffman, 1994), the 1:1 or "tight-binding" complex predominates in equimolar solutions of the two proteins at low salt, and it can be inferred from published data that the *in vitro* electron-transfer-active species at physiological ionic strengths are 1:1 complexes. These complexes are believed to be the electron-transfer intermediates in the CCP-catalyzed oxidation of ferrocytochrome *c* by hydrogen peroxide (Poulos & Kraut, 1980; Bosshard et al., 1991). As such, they represent a prototype for studies of many different metalloprotein redox complexes that occur in mitochrondria. Three types of CCP complexes have been studied: those formed with horse, tuna, and yeast cytochromes *c*. Whereas the complex with yeast Cytc is the only physiologically relevant one, the tuna Cytc complex was originally modeled with CCP (Poulos & Kraut, 1980), and the horse Cytc complex has received the most extensive experimental attention (McLendon, 1988; Wallin et al., 1991).

Only recently, with publication of the crystal structures of the CCP/horse Cytc and CCP/yeast Cytc complexes (Pelletier & Kraut, 1992), has there been a solid structural basis for interpreting much of the spectroscopic and kinetic work published on these complexes (see Figure 1). Those studies defined many solution-state properties of the complexes relevant to our current investigation. First, they showed clearly that tight 1:1 complexation between CCP and horse Cytc occurs in low-salt solutions ($\mu < 20$ mM), with association constants reported to vary between 6×10^6 M^{-1} ($\mu = 10$ mM) and 2.2×10^3 M^{-1} (high salt: $\mu = 200$ mM) (Erman & Vitello, 1980). Second, they indicated that CCP exhibits a larger affinity for ferrous cytochromes *c* than ferric cytochromes *c* under low ionic strength conditions (Leonard & Yonetani, 1974; Moench et al., 1987), and the relative affinity of CCP to ferrous vs ferric cytochromes *c* is reversed in the high-salt solution ($\mu > 100$ mM) (Mauk et al., 1994). Third, they indicated that interprotein electron transfer within the CCP/Cytc complexes is dependent on steric factors and electrostatic conditions (Hoffman et al., 1990; McLendon, 1991; Tollin & Hazzard, 1991; Geren et al., 1991; Hahm et

† This work was supported by NIH Grants GM33330 (M.R.O.), GM45986 (J.D.S.), and GM 48714 (D.L.R.).

* Authors to whom correspondence should be addressed.

‡ AT&T Bell Laboratories.

§ University of Hawaii.

|| Current address: Department of Chemistry, University of Denver, Denver, CO 80208.

⊥ Washington State University.

University of New Mexico.

⊗ Abstract published in *Advance ACS Abstracts,* December 15, 1995.

[1] Abbreviations: CCP, cytochrome *c* peroxidase; Cytc, cytochrome *c*; CCO, cytochrome *c* oxidase; Mb, myoglobin; Hb, hemoglobin; RRS, resonance Raman spectroscopy; RDS, Raman difference spectroscopy; CD, circular dichroism; CCD, charge-coupled device; TRS, transient Raman spectroscopy; NMR, nuclear magnetic resonance; CW, continuous wave; UV, ultraviolet; CO, carbon monoxide; CN^-, cyanide; 5C/HS, pentacoordinate high spin; 6C/LS, hexacoordinate low spin.

0006-2960/96/0435-453$12.00/0

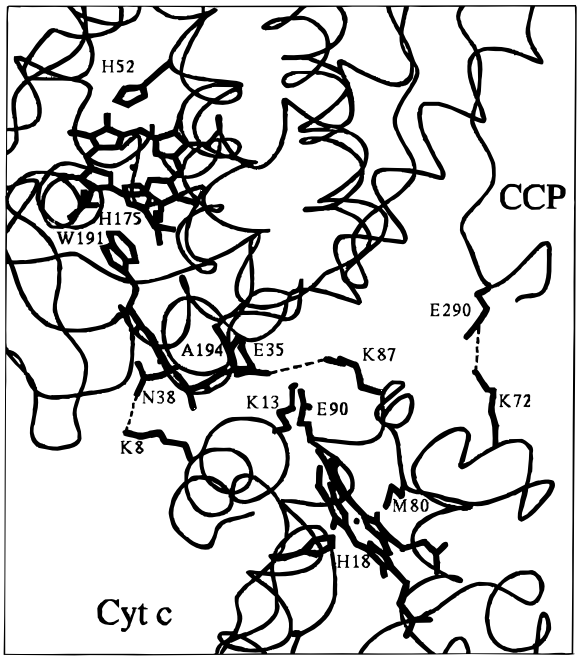

FIGURE 1: Crystal structure of yeast cytochrome *c* peroxidase (top left) electrostatically complexed with horse cytochrome *c* (bottom right), reported by Pelletier and Kraut (1992). The coordinates were obtained from the Brookhaven Protein Data Bank and displayed with Quanta software from Molecular Simulation Inc. His-52 resides above the heme (top right) of CCP at neutral pH (unligated) but moves closer and coordinates to the heme iron at alkaline pH and in some site-directed mutants. The electron-transfer pathway (Trp-191···Gly-192···Ala-193···Ala-194) proposed by Pelletier and Kraut (1992) links the proximal region of the heme of CCP to the interface of the two proteins. The three lysine groups from cytochrome *c* (Lys-8, Lys-87, and Lys-72) form hydrogen-bonding interactions with Asn-38, Glu-35, and Glu-290 from CCP, respectively. In the CCP/Cytc complex, Lys-13 and Glu-90 from horse cytochrome *c*, which are near the interface of the two proteins, also change their conformation.

al., 1992). This implies that electron transfers within the catalytic mechanism of CCP are likely to be dependent on both the local environment of the heme-active site and on more global changes in protein structure. For example, the CCP T191F mutant readily forms an electrostatic complex with cytochrome *c* but shows no catalytic function (Mauro et al., 1988; Miller et al., 1988). Moreover, the A193F mutation presumably disrupted the proposed interprotein electron-transfer pathway involving Trp-191···Gly-192···Ala-193···Ala-194 and thus resulted in a 2−4-fold decrease in the catalytic rate of CCP (Miller et al., 1994a). Therefore, in order to assess the relative importance of these two factors, it is highly desirable to obtain information directly concerning the equilibrium active site geometries as well as the structural dynamics that accompany catalytic and electron-transfer functions of CCP.

The choice of resonance Raman spectroscopy (RRS) is logical because it is a powerful technique for determining biostructures and dynamics (Spiro, 1988; Wang et al., 1995a). More importantly for this research is its unique capability of selectively and sensitively reporting on the heme-active sites of both CCP and Cytc. For example, previous RRS studies have revealed a variety of heme pocket alterations induced by CCP mutagenesis (Smulevich et al., 1991; Spiro et al., 1990; Smulevich, 1993), solution conditions (Shelnutt et al., 1983; Hashimoto et al. 1986; Dasgupta et al., 1989; Smulevich et al., 1989; Wang et al., 1992a−c), and even protein aging (Dasgupta et al., 1989). RRS is thus capable of providing a selective view of structural and dynamic consequences of electrostatic complex formation at the proteins' active sites. Recently, Hildebrandt et al. (1992) examined the effects of ferric CCP complexation with yeast and horse heart cytochromes *c* using spectral deconvolution to quantify the behavior of the overlapping RR spectra of the heme active sites of the two proteins. They concluded that complexation induces an up to 20% increase in the population of the six-coordinate low-spin (6C/LS) form of the CCP heme. They also inferred that changes in the conformation at the peripheral side chains of the CCP heme occurred upon yeast Cytc binding.

In this study we reexamine the effects of the formation of the CCP/Cytc complexes on the heme environment as well as the protein secondary structure of the two proteins by using RRS, Raman difference spectroscopy (RDS), and circular dichroism (CD) and by probing the photodynamics of the CCP active site via transient Raman spectroscopy (TRS). The data from the CCP/Cytc complexes are carefully compared with those from the uncomplexed mixtures, instead of those from isolated proteins. Our spectra do not confirm the findings of Hildebrandt et al. (1992). In fact, they show no change in either the distal or proximal heme environment of the yeast CCP upon complexation with cytochrome *c*. In addition, the data from the carbon monoxide derivative of CCP clearly indicate a similar active site in the complexes with cytochrome *c* and the uncomplexed mixtures. Moreover, our results extend prior studies of CCP/Cytc complexes (Pelletier & Kraut, 1992) by investigating the formation of the CCP/Cytc complexes in a variety of redox states [e.g., CCP(III)/Cytc(III), CCP(III)/Cytc(II), and CCP(II)/Cytc(II)]. Finally, all the studies of the CCP/Cytc complexes are carried out in solution, thereby offering an excellent model of CCP/cytochrome *c* complexes under physiological conditions.

MATERIALS AND METHODS

Sample Preparation. Cytochrome *c* (horse heart type VI) was purchased from Sigma Chemical Co. and used without further purification. Cytc was oxidized to the ferric state with an excess of potassium ferricyanide followed by passage through a small Dowex 1-X8 (Bio-Rad) column previously equilibrated with 5−10 mM Mes buffer, pH 6.8. Yeast CCP was isolated and purified from baker's yeast (Red Star) by a modified procedure of Yonetani (Moench, 1986; Wang, 1992). Great care was taken to use fresh CCP in all experiments to avoid any conformational and spin-state changes caused by the aging of the protein (Dasgupta et al., 1989; Anni & Yonetani, 1992). Ferrous CCP or Cytc was made by the anaerobic addition of a 10-fold excess of sodium dithionite (Aldrich) solution to the sample that was previously degassed in sealed optical cells. The concentrations of CCP(III) and Cytc(III) were monitored spectroscopically at 408 and 410 nm by using extinction coefficients of 93 (Yonetani & Ray, 1965) and 106.1 mM^{-1} cm^{-1} (Margoliash & Frohwirt, 1959), respectively.

The electrostatic complexes of CCP(III)/Cytc(III) (at low ionic strength) were prepared, at 4 °C, by mixing a 1:1 molar ratio of the CCP(III) and Cytc(III) samples in 5−10 mM Mes, pH 7.0, or Tris-HCl, pH 8.5. A small (4−6%) increase in the intensity of the composite Soret band (trace g in Figure 2) (Erman & Vitello, 1980) serves as an indication of

complex formation. The CCP(III)/Cytc(II) complex was produced by flushing a nitrogen atmosphere over 150−200 μL of the CCP(III)/Cytc(III) complex solutions, followed by a selective reduction of Cytc(III) (to ferrous Cytc) via a 3-fold excess of 10 mM ascorbic acid (Aldrich) stock buffer solution. The CCP(II)/Cytc(II) complex was produced via a similar procedure except that a 3−5-fold excess of sodium dithionite solution, instead of ascorbic acid, was anaerobically added to the CCP(III)/Cytc(III) complex. The CCP/Cytc complex solutions made at each redox state were then split into two samples with equal volume. One of them was used to prepare the uncomplexed mixture (at high ionic strength) of CCP/Cytc (control) by adjusting the buffer concentration from 10 to 200 mM with 1 M Mes, pH 7.0, or 1 M Tris-HCl, pH 8.5. The same volume of 10 mM Mes, pH 7.0, or 10 mM Tris-HCl, pH 8.5, was then added to the second sample (complex) in order to minimize the spectral deviations from the dilution-induced difference in the protein concentration between the two samples (complex and mixture). To make the complex and mixture of CCP(II)−CO/Cytc(II), natural (Matheson) and isotopically labeled CO (ICON) were introduced into the CCP(II)/Cytc(II) samples, respectively. The absorption spectra of all the samples, including the isolated proteins, complexes, and uncomplexed mixtures, were checked both prior to and after Raman measurements to confirm their integrity, as well as assure the absence of unexpected changes of the samples by laser irradiation.

Spectroscopic Measurements. The instrumentation for resonance Raman measurements (Figures 6−8) has been described elsewhere (Wang et al., 1994, 1995a). In order to avoid the photogenerated heme reduction of horse Cytc-(III) or the CO dissociation of CCP(II)−CO adducts, a combination of a high-performance charge-coupled device (CCD) camera (Princeton Instrument) and an extremely low CW laser power (from 0.3 to 0.6 mW over the samples) was employed. Tens of 1-min spectra were recorded and averaged to improve the signal to noise ratio. The frequencies of the Raman-shifted lines were calibrated against the lines from indene, acetone (1709.7 cm^{-1}), and $K_4Fe(CN)_6$ (2056.7 and 2091.7 cm^{-1}) standards. Raman difference spectroscopy (Figures 4 and 5) was carried out by using a divided Raman difference cell and a dual channel Raman spectrometer described elsewhere (Shelnutt et al., 1979; Rousseau, 1981). The 406.7 and 413.1 nm lines from a krypton ion laser (Spectra Physics) and the 441.6 nm line from a helium−cadmium laser (Liconix) were employed as the excitation sources.

Transient resonance Raman spectra (Figures 3A and 10) were recorded with instrumentation described in detail elsewhere (Wang, 1992). The data were obtained by using ∼10-ns pulses and a combination of focusing optics and/or neutral density filters to control photon flux at the samples (3×10^6−2.5×10^8 W/cm^2). The excitation wavelengths of 406−408, 420−422, and 436−440 nm from a nitrogen-pumped dye laser (Molectron UV-24/DL14) were used to selectively enhance specific chromophores in the complexes.

Optical absorption and circular dichroism (CD) spectra were measured on a Hewlett-Packard HP8452A diode array UV/vis spectrometer and a JASCO J-600 spectropolarimeter, respectively, under the same conditions as those used for the resonance Raman investigations. Measurements of the reoxidation of photoreduced CCP within the CCP(III)/Cytc-(II) complexes and mixtures were made by first photoreducing the samples with an N_2 dye laser (high power) at 410 nm, followed by the measurement of absorption changes at the Soret maximum of the CCP(III) low-spin heme (414 nm) (Wang et al., 1992c).

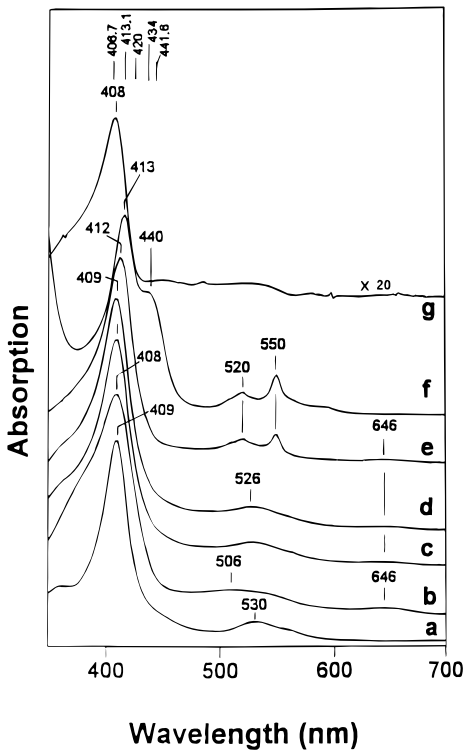

FIGURE 2: Optical absorption spectra from (a) Cytc(III), (b) CCP-(III), (c) uncomplexed mixture and (d) complexed form of CCP-(III)/Cytc(III) (1:1 ratio), and complexed forms of (e) CCP(III)/Cytc(II), and (f) CCP(II)/Cytc(II). Buffer solutions: (a, b, d−f) 10 mM, and (c) 200 mM Mes, pH 7.0. Trace g is the difference of the complex (trace d) minus the uncomplexed mixture (trace c) of CCP(III)/Cytc(III) with an 1:1 subtraction. It shows a net increase (∼5%) in the absorbance of the composite Soret upon the complexation of the two proteins. Above the spectra the laser excitation wavelengths utilized in the present study are listed. The frequencies were selected to optimize the resonance effect.

RESULTS

Effects of Complexation. The optical absorption spectra of the CCP(III)/Cytc(III) complex (trace d) and its uncomplexed mixture (trace c) at neutral pH are depicted in Figure 2. The observable difference, upon 1:1 subtraction, is a small (∼5%) increase in the intensity of the composite Soret band by the complexation (trace g). This effect has been observed previously (Erman & Vitello, 1980) and serves as an indication of complex formation. Subtraction, with a changing ratio, between spectra from the CCP(III)/Cytc(III) complex and mixture is unable to balance out the small increase in the Soret intensity but produces a difference spectrum (not shown) with a maximum at 406 nm and a minimum at 426 nm. It should be noted that this behavior does not corroborate the ∼10% ligation-state conversion of CCP(III) heme [from pentacoordinate high spin (5C/HS) to 6C/LS] previously reported by Hildebrandt et al. (1992) since for such a change a difference spectrum with an inverse pattern (a minimum near 406 nm and a maximum near 420 nm) would be expected. In addition, the difference spectrum resembles neither the difference between the complexes of CCP(III)/Cytc(II) and CCP(III)/Cytc(III) nor that of CCP-(III) minus Cytc(III). In all other respects, the absorption

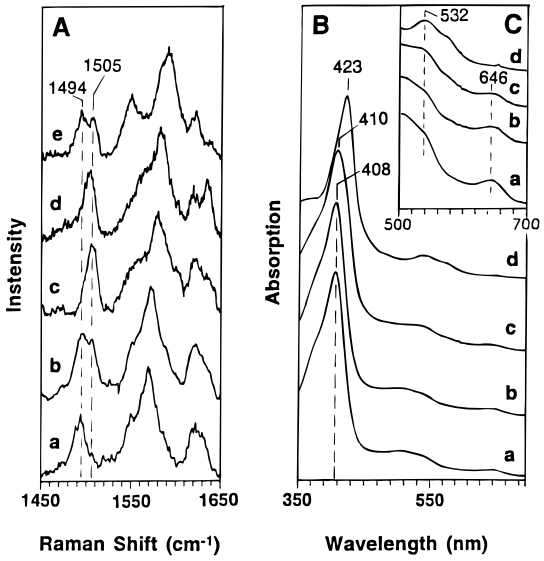

FIGURE 3: (A) Transient resonance Raman data of fresh yeast CCP(III) in 100 mM phosphate buffer, pH 7.0, containing (a) no $K_3Fe(CN)_6$ and (b) 1 equiv and (c) 2 equiv of $K_3Fe(CN)_6$. Spectra d and e are those for CCP(III)/Cytc(III) and CCP(III)/Cytc(II) complexes (in 10 mM Mes buffer, pH 7.0) in the presence of $K_3Fe(CN)_6$. All the spectra were obtained with an excitation wavelength of 408 nm. In trace d, a single peak of ν_3 at 1505 cm^{-1} indicates the overlap of the signals of 6C/LS ferric hemes from both proteins. ν_3 of low-spin cytochrome *c* shifts to 1494 cm^{-1} in trace e due to the heme reduction. (B, C) Optical absorption spectra of 50 μM fresh CCP(III) in 100 mM phosphate, pH 7.0, with no $K_3Fe(CN)_6$ (a) and 50 μM $K_3Fe(CN)_6$ (b), prior to the laser illumination. Spectra c and d are from samples containing 50 μM (c) and 100 μM $K_3Fe(CN)_6$ (d), respectively, but observed after laser illumination.

spectra of the complexes are coincident with those of relevant mixtures. Specifically, the CCP(III)/Cytc(III) complex (spectrum d) and mixture (spectrum c) both exhibit Soret bands at 409 nm and broad bands at 526 nm corresponding to the sum of Q bands of CCP(III) at 504 nm and Cytc(III) at 530 nm. Similar correspondence was also observed for the absorption spectra of mixtures and complexes of CCP(III)/Cytc(II) and CCP(II)/Cytc(II) (traces e−f). The near coincidence of spectra of CCP/Cytc complexes with those of their uncomplexed mixtures indicates that the electronic properties of the heme sites of CCP and Cytc are not significantly perturbed by complexation.

In our earlier efforts to prepare the samples of CCP(III)/Cytc(III) with completely oxidized cytochrome *c*, a small amount of potassium ferricyanide was found to remain in the Cytc(III) sample even after column chromatography (Sephadex G-25) (Wang et al., 1990a). The residue of ferricyanide does not affect the absorption spectrum prior to the laser irradiation (traces b in Figure 3B,C). However, laser excitation of the samples containing residual ferricyanide does substantially alter the optical spectra of ferric CCP (see spectra c and d in Figure 3B,C) and the resonance Raman spectra of isolated CCP(III) (traces b and c in Figure 3A) and its complexes with cytochrome *c* (traces d and e in Figure 3A). This is evidenced by a red shift of the Soret maximum of CCP(III) from 408 to 423 nm and an increase in the intensity of a Raman spin-state marker, ν_3, at 1505 cm^{-1}, indicating the direct conversion of a 5C/HS heme to a 6C/LS heme of ferric CCP. We attribute this to the coordination of 5C/HS heme in ferric CCP by CN^- generated by the laser-induced photodissociation of ferricyanide.

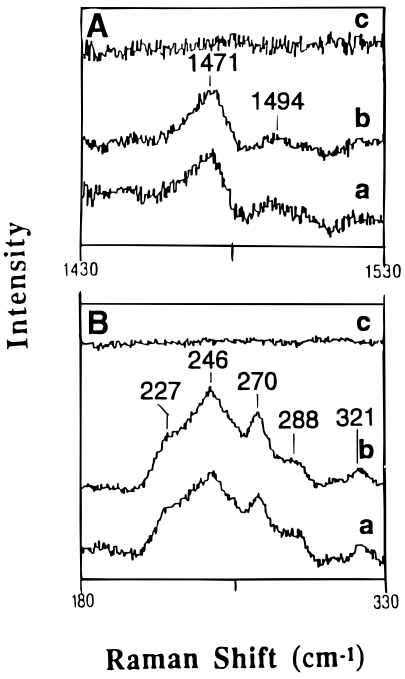

FIGURE 4: Raman difference spectra of CCP(II)/Cytc(II) (1:1 molar ratio) dissolved in (a) 200 mM (uncomplexed mixture) or (b) 10 mM Mes buffer, pH 7.0 (complex), in the (A) spin-state marker ν_3 and (B) iron−histidine stretching (ν_{Fe-His}) regions. Trace c in each region is the difference of complex minus mixture. Spectra are the averages of six to eight scans and were obtained with low-power (~5 mW over the samples) CW excitation at 441.6 nm.

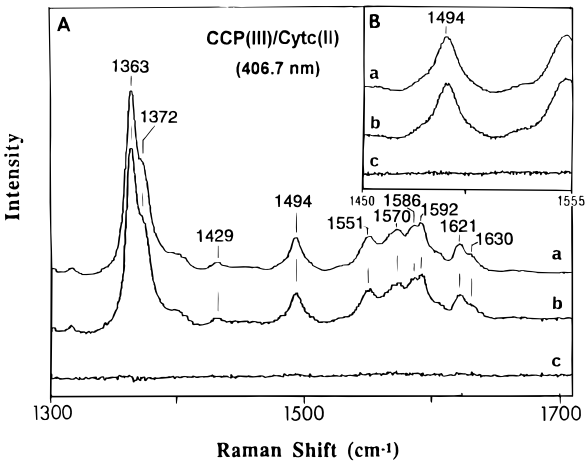

FIGURE 5: Raman difference spectra of CCP(III)/Cytc(II) (1:1 molar ratio) in (a) 10 mM (complex) and (b) 200 mM Mes buffer, pH 7.0 (uncomplexed mixture), recorded in (A) high-frequency and (B) spin-state marker ν_3 regions. Trace c in each region is the difference of complex minus mixture. Spectral conditions were the same as in Figure 4 except 406.7 nm excitation was used.

Equilibrium Structure Detected by RRS and RDS. Our RRS data further probe the local structural environments of the heme sites in CCP and cytochrome *c*. Figures 4−6 compare the spectra of CCP(II)/Cytc(II), CCP(III)/Cytc(II), and CCP(III)/Cytc(III), respectively, under high ionic strength (uncomplexed mixture) and low ionic strength conditions (complexed). Spectra of CCP/Cytc complexes show varying contributions of each chromophore at the specific excitation wavelengths used. CCP(III), CCP(II), Cytc(III), and Cytc(II) exhibit maxima in their Soret absorption bands at 408, 440, 410, and 414 nm, respectively, and thus contribute significantly to spectra obtained at those excitation wave-

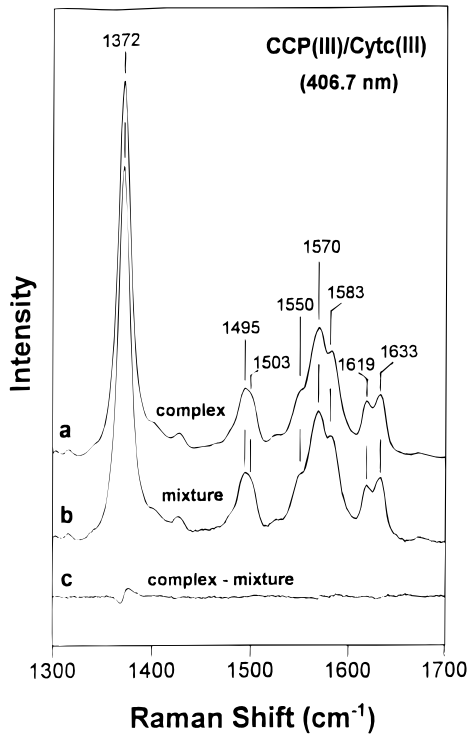

FIGURE 6: Resonance Raman spectra of CCP(III)/Cytc(III) (1:1 molar ratio) in (a) 10 mM (complex) and (b) 200 mM Mes buffer, pH 7.0 (uncomplexed mixture), recorded in the high-frequency region. Trace c is the difference spectrum of complex minus mixture. In order to minimize the photoinduced reduction of Cytc-(III) heme, or coordination of CCP(III) heme iron by CN^- which was generated from residual ferricyanide by the laser, an extremely low CW laser power (0.3−0.6 mW) and a high-performance CCD detector were utilized here.

lengths, respectively. For instance, RDS studies of CCP-(II)/Cytc(II) using 441.6 nm excitation yield spectra dominated by the CCP(II) heme (Figure 4). Specifically, the strong peak of ν_3 (see Figure 4A) at 1471 cm^{-1} is from the 5C/HS ferrous heme of CCP while the contribution from low-spin Cytc(II) at 1494 cm^{-1} is quite small.

Our data convincingly demonstrate that the equilibrium properties of the CCP heme are not perturbed in the CCP-(II)/Cytc(II) complex. Conversion of the ferrous CCP heme from 5C/HS to 6C/LS should be readily observed by the relative intensities of ν_3 at 1471 and 1494 cm^{-1} (Wang et al., 1992a) though ν_3 from low-spin CCP(II) is coincident with that for Cytc(II) at 1494 cm^{-1}. The stability of CCP's equilibrium structure upon the complexation is also evident from the Raman data in the iron−histidine stretching frequency (ν_{Fe-His}) region (Figure 4B). The frequency and the intensity of ν_{Fe-His} mode are sensitive to the proximal ligand properties and its interactions with the heme moiety (Kitagawa, 1988). The absence of the line at 307 cm^{-1} from Cytc(II) confirms that our spectra are dominated by ferrous CCP, and the contributions from Cytc(II) are also negligible in the low-frequency region (Cartling, 1988). The spectra of CCP(II), both from its complex (trace b) and mixture (trace a), are virtually identical to those from isolated CCP(II) reported by other groups (Hashimoto et al., 1986; Dasgupta et al., 1989; Spiro et al., 1990), displaying the two components of ν_{Fe-His} at 246 cm^{-1} and a shoulder at 227 cm^{-1}.

Figure 5 shows RDS spectra of free (trace b) and complexed CCP(III)/Cytc(II) (trace a). The heme oxidation states were confirmed by the positions of ν_4, an oxidation-state marker, at 1363 cm^{-1} (ferrous Cytc) and 1372 cm^{-1} (ferric CCP), respectively. Here again there is no detectable difference between the high and low ionic strength samples. Under these conditions, the ν_3 lines from both Cytc(II) (6C/LS) and CCP(II) (5C/HS) coincide at ∼1494 cm^{-1} (see Table 1). Spectra obtained at higher signal to noise ratio in the ν_3 region (1450−1555 cm^{-1}) confirm the absence of a change in spin state of either heme (see Figure 5B).

The studies of CCP(III)/Cytc(III) were complicated by the contamination from auto- or photoinduced heme reduction of cytochrome *c*. The addition of ferricyanide to the CCP-(III)/Cytc(III) sample completely oxidized the Cytc heme; however, as mentioned above, the direct coordination to the CCP(III) 5C/HS heme of the photodissociated CN^- from ferricyanide produced a variable amount of low-spin CCP heme (Wang et al., 1990a; Hildebrandt et al., 1992; also see spectra d and e in Figure 3). This artifact could be removed if Cytc(III) containing a very slight excess of ferricyanide was passed through a Dowex 1-X8 column prior to its complexation with ferric CCP. In addition, the use of the high-performance CCD detector allowed spectra to be obtained under the extremely low CW laser power (0.3−0.6 mW), thus minimizing the photodissociation of any trace amount of ferricyanide that might have survived the chromatography. The resulting RR spectra are shown in Figure 6. Spectra from both the complex (a) and mixture (b) of CCP(III)/Cytc(III) display a sharp and symmetric ν_4 at 1372 cm^{-1}, indicating that both hemes are completely oxidized. Since the excitation (406.7 nm) slightly favors the resonance enhancement for ferric CCP (408 nm) over that for Cytc-(III) (410 nm), the contributions from ferric Cytc (ν_3, 1503 cm^{-1}; ν_2, 1583 cm^{-1}) thus appear as the shoulders of the stronger ferric CCP bands (ν_3, 1495 cm^{-1}; ν_2, 1570 cm^{-1}). While the small difference in the composite ν_4 band may indicate a slight alteration of the electronic structure of at least one of the hemes, it could also result from a small artifactual alignment difference between the two samples. However, we were unable to reproduce the results by other investigators (Hildebrandt et al., 1992) who reported an ∼10% increase in the population of CCP(III)'s 6C/LS heme by forming a complex with cytochrome *c*.

Carbon Monoxide Derivatives. The RR spectra of the carbon monoxide adducts from isolated CCP(II) (trace a), the complexes (traces c and d), and the uncomplexed mixture (trace b) of CCP(II)/Cytc(II) were recorded in the low-(Figure 7) and high-frequency (Figure 8) regions. Our low-frequency spectrum from the $^{12}C^{16}O$ adduct of isolated CCP-(II) (a) confirms the previous results reported by Spiro and Rousseau groups (Evangelista-Kirkup et al., 1986; Dasgupta et al., 1989), showing lines at 534 and 589 cm^{-1} for Fe−CO stretching (ν_{Fe-CO}) and Fe−C−O bending (δ_{Fe-C-O}) modes, respectively. The frequencies for those marker lines, which are more evident in the difference spectrum (trace e) of CCP(II)−$^{12}C^{16}O$ (trace a) minus CCP(II)−$^{13}C^{18}O$ (data not shown), are quite high, and the ratio in the intensities of δ_{Fe-C-O} vs ν_{Fe-CO} ($I_{\delta_{Fe-C-O}}/I_{\nu_{Fe-CO}}$) is greater in comparison to other heme proteins such as hemoglobin and myoglobin (Wang et al., 1995b). The spectra from the $^{12}C^{16}O$−CCP-(II) in the complex (spectrum c) and mixture (spectrum b) are complicated by scattering from Cytc(II) at this excitation. However, the difference spectrum (trace f) of $^{12}C^{16}O$−CCP-(II) (trace c) minus $^{13}C^{18}O$−CCP(II) (trace d) from the CCP

Table 1: Some Important Marker Lines (in cm^{-1}) from RR Spectra of Yeast CCP and Horse Cytc

	ν_4	ν_3	ν_2	ν_{10}	$\nu_{C=C}$	ν_{Fe-CO}	ν_{Fe-C-O}	ν_{C-O}	ν_{Fe-His}	ref
Isolated proteins										
CCP(III), pH 7.0	1372	1495	1570	1629	1620					*c*−*e*, *g*−*i*
CCP(III), pH ∼9	1375	1505	1579	1637	1624					*c*−*e*, *g*
CCP(III), pH 7.0	1356	1471	1563	1604	1618				227/246	*c*, *d*, *i*−*k*
CCP(II), pH ∼9	1360	1495	1581	1620	1628					*c*, *d*, *j*, *m*
CCP(II)−CO, pH 6	1372	1496	1577	1629	1615	535	589	1921.5		*b*, *c*, *f*, *h*, *i*
Cytc(III)	1375	1504	1584	1636						*d*, *l*
Cytc(II)	1363	1494	1585/1592	1622						*d*, *l*
complexes										
CCP(III)/Cytc(III), pH 7.0	1372^a	$1495_p/1503_c$	$1570_p/1583_c$	1633	1619_p					*c*
CCP(III)/Cytc(III), pH 8.5	1375	1504	1583	1636						*c*
CCP(III)/Cytc(II), pH 7.0	$1372_p/1363_c$	1494	$1570_p/1586\&1592_c$	$1630_p/1621_c$	1621_p					*c*
CCP(II)/Cytc(II), pH 7.0	1355_p	$1471_p/1494_c$	1564_p		1604_p				227/246	*c*
CCP(II)/Cytc(II), pH 8.5	1360_p	$1471_p/1494$								*c*
CCP(II)−CO/Cytc(II), pH 6	$1372_p/1362_c$	1492	$1578_p/1590_c$	1629_p	1616	535.5	589	1921.5		*c*

[a] The subscripts p or c used here designate the assignment of the line(s) as originating from CCP (p) or cytochrome *c* (c), respectively, while the data containing no subscript are the contributions from both proteins. [b] Wang et al., 1995b. [c] This work. [d] Wang, 1992. [e] Hashimoto et al., 1986. [f] Satterlee & Erman, 1984. [g] Wang et al., 1992c. [h] Smulevich, 1993. [i] Dasgupta et al., 1989. [j] Wang et al., 1992a. [k] Spiro et al., 1990. [l] Cartling, 1988. [m] Smulevich et al., 1989.

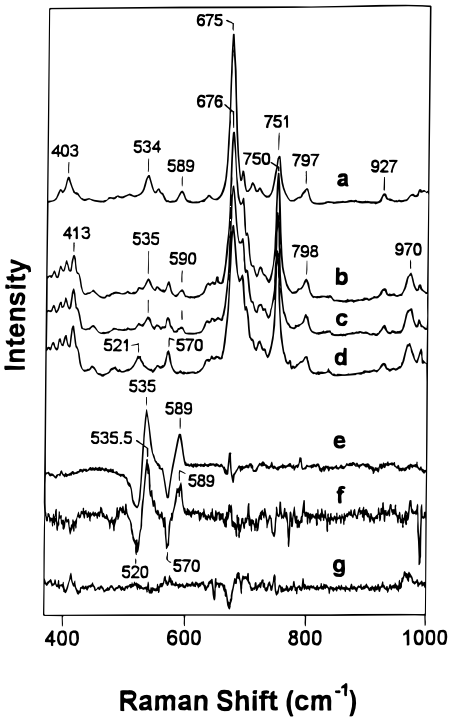

FIGURE 7: Resonance Raman spectra in the low-frequency region of the $^{12}C^{16}O$ adducts of (a) isolated CCP(II) (in 10 mM Mes, pH 6.7), (b) uncomplexed mixture (in 200 mM Mes, pH 6.7), and (c) complexed form (in 10 mM Mes, pH 6.7) of CCP(II)/Cytc(II). Spectrum d is the $^{13}C^{18}O$ derivative of the CCP(II)/Cytc(II) complex (in 10 mM Mes, pH 6.7). Traces e and f are the difference spectra of $^{12}C^{16}O$-bound forms minus $^{13}C^{18}O$-bound forms from isolated CCP(II) (e) and from the complex (f) of CCP(II)/Cytc(II) (trace c and trace d), respectively. Trace g is the difference of the spectrum from the $^{12}C^{16}O$-bound derivative of the CCP(II)/Cytc(II) complex (trace c) minus that from the corresponding mixture (trace b). The data were recorded under extremely low CW laser power (<0.3 mW) (excitation: 413.1 nm) to minimize the photodissociation of carbon monoxide from the heme iron of CCP(II).

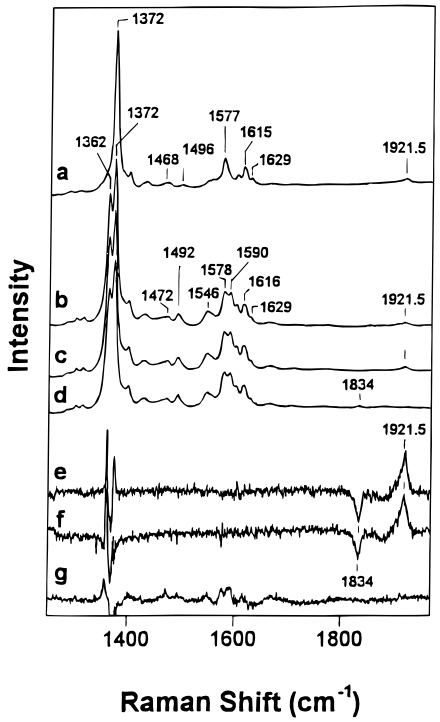

FIGURE 8: Resonance Raman spectra in the high-frequency region of the $^{12}C^{16}O$ adducts of (a) isolated CCP(II) (in 10 mM Mes, pH 6.7), (b) uncomplexed mixture (in 200 mM Mes, pH 6.7), and (c) complexed form (in 10 mM Mes, pH 6.7) of CCP(II)/Cytc(II). Spectrum d is the $^{13}C^{18}O$ derivative of the CCP(II)/Cytc(II) complex (in 10 mM Mes, pH 6.7). Traces e and f are the difference spectra of the $^{12}C^{16}O$-bound forms minus the $^{13}C^{18}O$-bound forms from isolated CCP(II) (e) and from the complex (f) of CCP(II)/Cytc(II) (trace c and trace d), respectively. Trace g is the difference of the spectrum from the $^{12}C^{16}O$-bound derivative of the CCP(II)/Cytc-(II) complex (trace c) minus that from the corresponding mixture (trace b). The experimental conditions used were the same as shown in Figure 7.

(II)/Cytc(II) complex resembles that from isolated CCP(II) (trace e) in both the position and $I_{\delta_{Fe-C-O}}/I_{\nu_{Fe-CO}}$, suggesting that the ligand binding geometry of CCP(II) is unaffected by the complexation with Cytc(II). This similarity was further confirmed by the coincidence (see trace g) of the spectrum from the $^{12}C^{16}O$ adduct of the CCP(II)/Cytc(II) complex with that of corresponding mixture.

The sharp line from ν_4 at 1372 cm^{-1} in the $^{12}C^{16}O$ adduct of isolated CCP(II) (spectrum a in Figure 8) indicates that the photodissociation of carbon monoxide is very limited under the laser powers employed (Dasgupta et al., 1989). Thus, ν_3, ν_2, and ν_{10} from CCP(II)−$^{12}C^{16}O$ are able to be assigned at 1496, 1577, and 1629 cm^{-1}, respectively (see Table 1). The C−O stretching mode (ν_{C-O}) located at 1921.5 cm^{-1}, as previously reported in infrared studies (Satterlee

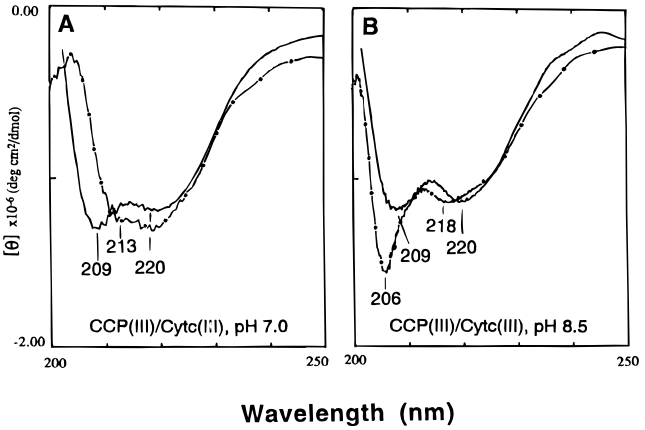

FIGURE 9: Circular dichroism spectra of CCP(III)/Cytc(III) (1:1) complexes (—) and uncomplexed mixtures (—•—) in the far-UV region. (A) 10 mM (—) and 200 mM (—•—) Mes, pH 7.0, and (B) 10 mM (—) and 200 mM (—•—) Tris-HCl, pH 8.5, were employed to prepare the complex and mixture, respectively.

& Erman, 1984), was identified by the isotopic substitution of CO [trace e: CCP(II)−$^{12}C^{16}O$/CCP(II)−$^{13}C^{18}O$]. This maker line is detectable in the spectra of the CO adducts in the CCP(II)/Cytc(II) complex (traces c and d) and in the mixture (trace b). Here again, the isotope difference spectra for the complex are nearly identical to those of the mixture, confirming that complexation does not perturb the distal heme pocket of CCP(II).

Tertiary Structure of the CCP/Cytc Complexes. It is well established that circular dichroism (CD) signals (particularly in the far-UV region) are susceptible to the overall protein tertiary or secondary structure (Myer, 1985). Indeed, the sensitivity of the protein structure of CCP(III) and Cytc(III) to complexation and pH is apparent in the CD spectra depicted in Figure 9. In spite of the similar heme moiety inferred by the Raman data, the far-UV CD spectra of CCP(III)/Cytc(III) complexes are quite distinct from those of the uncomplexed mixtures, at either pH 7.0 or pH 8.5. Specifically, at neutral pH the complex exhibits a negative ellipticity at 209 nm and a weak signal at 220 nm, while its uncomplexed mixture has a broad signal nm with a shoulder at 213 nm (Figure 9A). Elevation of the pH to 8.5 (Figure 9B) produces a slight intensification of the ellipticity at 220 nm in the CD spectra of the complex. The uncomplexed mixture of CCP(III)/Cytc(III), however, exhibits appreciable perturbations in the CD spectrum at the higher pH. These findings are consistent with the spectral changes reported from isolated CCP at elevated pH values (Wang et al., 1992a).

pH Dependence. The local heme environment of CCP is quite sensitive to solution pH. Both ferric and ferrous forms of the enzyme undergo a conversion from 5C/HS to 6C/LS heme as the pH is raised above 8.0 (Smulevich et al., 1989; Wang et al., 1992a−c). These pH−induced transitions are also observed in the RR spectra of the CCP(II)/Cytc(II) and the CCP(III)/Cytc(III) complexes (Figure 10). For instance, the intensity of the 6C/LS ν_3 of CCP(II) at 1494 cm^{-1} (vs the 5C/HS heme at 1471 cm^{-1}) at pH 8.5 (trace 10-a) significantly increases in comparison to that at neutral pH (trace 4A-b). For the CCP(III)/Cytc(III) complexes, while the spectrum at pH 7.0 (trace 6-a) is dominated by the 5C/HS heme of CCP(III) (ν_3 at 1495 cm^{-1}, ν_2 at 1570 cm^{-1}), the alkaline pH spectrum (trace 10-b) indicates a pH-induced

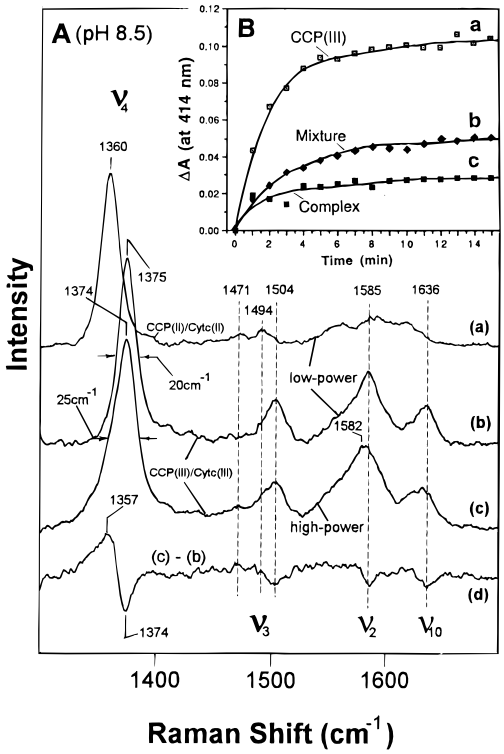

FIGURE 10: Resonance Raman spectra of CCP(II)/Cytc(II) (a) and CCP(III)/Cytc(III) (b−d) complexes in 10 mM Tris-HCl, pH 8.5. The samples were irradiated by (a, b) low (3×10^6−1×10^7 W/cm^2) and (c) high laser power [(1−2.5) × 10^8 W/cm^2]. Trace d is the difference of the spectrum from CCP(III)/Cytc(III) observed at high power (c) minus that at low power (b). The samples were excited at 434 nm for CCP(II)/Cytc(II) (a) and 410 nm for CCP(III)/Cytc(III) (b−d). (B) Reoxidation kinetics of photoreduced CCP at pH 8.5 from isolated CCP(III) (⊡) in 100 mM Tris-HCl, the 1:1 complex (■) (in 10 mM Tris-HCl), and the uncomplexed mixture (◆) (in 200 mM Tris-HCl) of CCP(III)/Cytc(II). Samples were irradiated by high laser power (∼2.5 × 10^8 W/cm^2) for ∼1 h under 4 °C, with the excitation wavelength at 410 nm (15 Hz) prior to the absorption measurement at 414 nm.

formation of the 6C/LS heme of CCP(III), resulting in a spectral overlap with that of low-spin Cytc(III) (ν_3 at 1504 cm^{-1}, ν_2 at 1585 cm^{-1}).

Ferric CCP has recently been shown to be readily photoreducible at alkaline pH (Wang et al., 1992c). The data presented in Figure 10 show that the CCP(III)/Cytc(III) complex exhibits similar behavior. Under low flux excitation, ν_4 at 1375 cm^{-1} and ν_3 at 1504 cm^{-1} (trace 10-b) clearly demonstrate the presence of the ferric heme of CCP (6C/LS). However, at high laser flux (trace 10-c), the asymmetric broadening of ν_4 ($\Gamma_{1/2}$, 25 cm^{-1}) and the weakening of signals from the 6C/LS ferric CCP (e.g., ν_3 at 1504 cm^{-1}, ν_2 at 1585 cm^{-1}, and ν_{10} at 1636 cm^{-1}), which are evident in their difference spectrum (trace 10-d), are all consistent with the photoreduction of CCP(III). In particular, the frequencies of ν_4 (1357 cm^{-1}) and ν_3 (1471 cm^{-1}, albeit weak) in the difference spectrum demonstrate that photoreduction of alkaline CCP(III) is followed by photolysis of the photoreduced 6C/LS heme to a 5C/HS heme as reported for the isolated CCP(III) (Wang et al., 1992c). In addition, the photoreduced CCP in the complex is slowly reoxidized in the absence of O_2 and redox mediators. This process can be easily monitored via absorption changes at 414 nm, and the results are plotted in Figure 10. While the yield of photoreduction of alkaline CCP(III) in complexes (trace c)

is lower than that of isolated CCP(III) (trace a) or CCP(III) in the uncomplexed mixture with Cytc(II) (trace b) under similar conditions, the lifetimes are quite similar.

DISCUSSION

Equilibrium Structures of CCP/Cytochrome c Complexes. Noncovalent complexes of yeast CCP and horse heart Cytc were prepared in our laboratories, where virtually all of the CCP and Cytc are electrostatically bound in a 1:1 stoichiometry when the ionic strength is less than 20 mM (Satterlee et al., 1987). The active site of cytochrome *c* in the CCP(III)/Cytc(III) complexes has been well characterized with proton NMR spectroscopy. The complexation between these proteins induces shift changes in the proton NMR spectrum of each of the ferricytochromes *c* studied to date (horse, tuna, and yeast isozymes 1 and 2). As a consequence of the formation of CCP/Cytc complexes, the hydrogen−deuterium exchange rates of certain amino acid amide protons located on the binding site of Cytc(III) are slowed down significantly (Yi et al., 1994). No evidence was found that complex formation with either Cytc(III) or Cytc(II) (from horse heart or tuna) induces any NMR spectroscopic changes in CCP, however, suggesting that Cytc binding at the CCP surface does not spectroscopically affect the CCP. The recently published crystal structure of the complex of ferric CCP (expressed in *Escherichia coli*) with ferric yeast iso-1-cytochrome *c* or with horse heart Cytc (see Figure 1) has confirmed the presence of the single binding site within the complexes of the two proteins and further revealed a possible electron-transfer pathway that follows the peroxidase backbone chain beginning at Ala-194 adjacent to the cytochrome *c* binding site and terminating with Trp-191 in the proximal heme pocket of CCP (Pelletier & Kraut, 1992). The fact that the catalytic rates of CCP are susceptible to the site-directed mutation of a residue involved in the electron-transfer pathway proposed from crystallography (e.g., A193F) (Miller et al., 1994a) but insensitive to mutations on other residues near the heme moiety (e.g., Y39F, Y42F, H181G, W223F and Y229F) strongly supports this proposal (Hahm et al., 1994). The CCP heme is in van der Waals contact with Trp-191, which has been demonstrated to be the site of an intermediate radical in the CCP catalytic cycle (Erman et al., 1989; Sivaraja et al., 1989; Hahm et al., 1992; Miller, 1994b). The crystal structures further revealed no large conformational changes in CCP, in particular, in its heme active site, in response to complexation with horse Cytc.

The RRS spectra obtained in this study confirm that complexation produces no dramatic changes in the local heme environment of CCP. This is true for all of the redox states examined in this investigation [CCP(II)/Cytc(II), CCP(III)/Cytc(II), and CCP(III)/Cytc(III); see Table 1]. The high-frequency RR spectra (Figures 4−6) are particularly sensitive to changes in the π*-electron density of the heme (reflected in the position of ν_4), iron-spin state (ν_3), or the geometry of the porphyrin macrocycle (ν_2, ν_3, ν_{10}, $\nu_{C=C}$). The spectra of the CCP(II)/Cytc(II) and CCP(III)/Cytc(II) complexes unequivocally establish that there are no dramatic changes in the heme geometry, ligation state, or electronic state that are induced by complexation. In order to avoid the contamination from auto- or photoreduction of the Cytc heme (in the absence of any oxidant) or from coordination of the CCP 5C/HS heme by photodissociated CN^- from ferricyanide (oxidant), great care was exercised to completely oxidize the cytochrome *c* in both complex and mixture samples, remove the slight excess of oxidant chromatographically, and obtain the RR spectra under extremely low CW laser power (0.3−0.6 mW) by using a high-performance CCD detector. Under these conditions, we were unable to reproduce the increase in the CCP(III) 6C/LS heme fraction previously reported by other researchers (Hildebrandt et al., 1992). Instead, our spectra of CCP(III)/Cytc(III) clearly indicate that the completely high-spin CCP heme is unaffected in both samples (complex and mixture; see Figure 6). We speculate that the presence of trace amounts of CN^-, photodissociated from the $K_3Fe(CN)_6$ used in the experiments of Hildebrandt et al. (1992), may account for the >10% increase in the 6C/LS fraction observed by them.

The maintenance of a 5C/HS heme active site in CCP is pivotal for its physiological function. It has been proved that this high-spin structure is sensitive to the hydrogen-bonding networks present in both the distal (Arg-48···His-52···Trp-51···His-181) and proximal sides (His-175···Arg-235···Trp-191) of the heme (Poulos & Finzel, 1984). Site-directed mutagenesis of some of these residues (Smulevich, 1993; Wang et al., 1990b) and pH-induced protein conformational perturbations (Smulevich et al., 1989; Wang et al., 1992a−c) resulted in a disruption of the hydrogen-bonding networks, thereby producing a 6C/LS heme species. However, the strong line of ν_3 at 1471 cm^{-1} from CCP(II) in its complex with Cytc(II) (trace 4A-b) and the similarities, in all the redox states, between the ν_3 lines from CCP/Cytc complexes (traces b in Figure 4A and traces a in Figures 5 and 6) and those from the uncomplexed counterparts (traces a in Figure 4A and traces b in Figures 5 and 6) demonstrate that CCP retains a 5C/HS heme in all of the complexes with Cytc (Table 1).

While our high-frequency RR data establish that no gross structural changes (such as spin-state conversion) at the CCP heme are engendered by Cytc complexation, the heme−ligand modes in the low-frequency spectra are expected to be sensitive to subtle structural perturbations of the proximal and distal heme pockets. To that end, we examined the ν_{Fe-His} (180−300 cm^{-1}) and ν_{Fe-CO} regions (450−600 cm^{-1}) of the RR spectra from the CCP(II)/Cytc(II) and CCP(II)−CO/Cytc(II) complexes, respectively. CCP(II) exhibits distinctive heme−histidine ligation behavior, as the hydrogen-bonding network of the CCP proximal heme pocket involves charge−charge interactions of Asp-235 and Trp-191 and the proximal ligand of the heme (His-175) that impart a sizable anionic character to His-175 (Poulos & Finzel, 1984). Such a unique H-bonded proximal histidine (imidazolate) is believed to be important in stabilizing the high positive charge [Fe(IV)═O] in the catalytic intermediate compound ES (Dasgupta et al., 1989; Finzel et al., 1991; Zhou, 1994) and is also expected to favor the Fe^{3+} over the Fe^{2+} state (Conroy et al., 1978). Indeed, an appreciable increase in the reduction potential has been detected from mutants of CCP where either the proximal ligand His-175 (Choudhury et al., 1994) or Asp-235 was replaced and thus the His-175···Asp-235···Trp-191 triad was disrupted (Goodin & McRee, 1993). No doubt the imidazolate character of His-175 imparted in the wild-type CCP strengthens the iron−histidine bond order. Two Raman lines have been identified as ν_{Fe-His} modes (Hashimoto et al., 1986; Dasgupta et al., 1989). Both occur at higher frequencies (227 and 246 cm^{-1}),

in comparison to those from neutral histidine-containing heme proteins such as Mb, Hb, and cytochrome *c* oxidase (CcO) (Kitagawa, 1988; Wang et al., 1995a). At alkaline pH or in a site-directed mutant where Asp-235 is replaced by an Asn residue, the two ν_{Fe-His} lines with higher frequencies disappear and a new ν_{Fe-His} line with a much lower frequency (205 cm^{-1}) becomes evident, indicating the disappearance of the imidazolate as a result of the disruption of its proximal H-bonding interactions (Spiro et al., 1990; Smulevich, 1993). The two ν_{Fe-His} lines from CCP(II) (227 and 246 cm^{-1}, Figure 3B) remain unperturbed upon the complexation with Cytc(II), providing additional evidence that the heme environment of CCP is the same in the complexes and the uncomplexed mixture.

Studies of CO adducts of heme proteins offer an important probe for the distal pockets of the heme catalytic active site and the interactions of heme-bound ligand with its environment (Ray et al., 1994; Wang et al., 1995a,b). CCP is unique in that the heme-bound CO is able to strongly interact with distal residues (Trp-51, Arg-48, and His-181) via H-bonding (Edwards & Poulos, 1990, Satterlee & Erman, 1984). Moreover, such H-bonding interactions offer remarkably high polar or steric effects on the bound CO, thereby influencing the geometry of Fe−C−O linkage (evident by the strong Fe−C−O bending mode at 589 cm^{-1}) and strengthening the Fe−CO bond (535 cm^{-1}) and weakening the C−O bond (1921 cm^{-1}) via the π back-donation from Fe d_π to C−O π^* orbitals (Ray et al., 1994; Wang et al., 1995a,b). It is anticipated that structural alterations in the distal heme active site of CCP induced by cytochrome *c* binding would affect these modes. We found that the three CO-associated marker lines obtained from the CCP(II)−CO/Cytc(II) complex are the same as those from the uncomplexed mixture or from isolated CCP(II) (Figures 7 and 8 and Table 1), reflecting a remarkably similar heme-active site for CCP.

In contrast to the behavior of the local heme environment, the spectroscopic data obtained in this study offer some evidence of small protein structural changes upon complexation. For instance, the formation of CCP(III)/Cytc(III) electrostatic complexes produces a small increase (∼5%) in the intensity of the composite Soret absorption band (Figure 2). This effect was noted previously by Erman and Vitello (1980). In addition, the binding of CCP with Cytc altered the Soret CD spectra eliciting a positive change in the ellipticity of the positive Cotton effect at 404 nm, which was attributed to changes in the protein−solvent interaction in the exposed front heme edge upon the complexation of the two proteins (Garber & Margoliash, 1994). We found that the complexation perturbed the far-UV CD spectra of the proteins as well (Figure 9). The optical activity in the far-UV region is dictated primarily by the changes in the protein tertiary and secondary structure (Myer, 1985). Thus, the systematic spectral alterations in this region strongly suggest that some form of protein conformational rearrangement accompanies complexation. However, in view of the RR spectra obtained in this study, it appears that these changes are limited to the surface amino acid residues and are not propagated to the heme-active sites. The behavior of the far-UV CD spectra is not unexpected since the crystal structure from the complex of CCP(III) with horse Cytc(III) reveals the existence of multiple interfacial conformations between the two proteins (Pelletier & Kraut, 1992). There are reported to be charge−charge interactions of Lys groups from cytochrome *c* (87, 72, and 8) with Glu (35 and 290) and Asn (38) from CCP, respectively (see Figure 1). Site-directed mutation of these residues in CCP resulted in either an appreciable suppression in the catalytic rates of CCP (Miller et al., 1994a) or a marked destabilization of its the reaction intermediate (Liu et al., 1995). Moreover, Pelletier and Kraut (1992) also found that the side chains of both Lys-13 and Glu-90 of horse cytochrome *c* in the complex moved significantly in accommodating the formation of intramolecular hydrogen bonding. Thus we conclude that the variations of CD data in the UV region (Figure 9) reflect changes involving the tertiary and secondary structure at the protein surfaces required for complexation. These, in turn, might be critical in reducing the outer reorganization energy and facilitating intracomplex electron transport between cytochrome *c* and CCP (Zhou, 1994).

Dynamics of CCP Active Site. While the recent crystallographic data of Pelletier and Kraut (1992) provide a compelling picture of the pathway for electron transfer within the CCP/Cytc complex (Figure 1), they do not directly yield the molecular mechanism for this process. It is quite likely that structural dynamics play a large role in regulating the rates and specificity of interprotein electron transfer. CCP/Cytc complexes exhibit large reorganization energies, λ, characteristic of heme proteins in general. A substantial fraction of λ is undoubtedly localized at the protein−protein interface. In view of the mutability of the CCP heme pocket in response to solution conditions, however, it can be anticipated that the structural dynamics of the heme pocket may contribute to λ and/or participate directly in "gating" electron flow. Our data demonstrate that, even though complexation minimally perturbs the equilibrium heme pocket structure, it does induce changes in the dynamics of the CCP active site.

It should not be too surprising that CCP is still capable of binding, albeit with lower affinity, to Cytc under mild alkaline conditions (<8.5). As mentioned above, the charge−charge interactions between CCP and Cytc involve the multiple H-bonding of Lys groups from cytochrome *c* (87, 72, and 8) with Glu (35 and 290) and Asn (38) from CCP, respectively (Figure 1). The disruption of electrostatic binding may take place under the conditions where all the Lys groups are deprotonated such as at a pH above its pK_a (∼10.0). Under mild alkaline conditions, CCP still maintains its electrostatic interactions with Cytc. We are unable to refute or confirm the possibility of two cytochrome *c* binding sites, at high pH (Pelletier & Kraut, 1992; Nuevo et al., 1993; Stemp & Hoffman, 1993; Zhou & Hoffman, 1994).

The complexation-induced restriction on the photodynamics of CCP is evident in the photoreduction process of alkaline CCP(III), though the previously reported heme coordination state conversion of isolated CCP (from 5C/HS to 6C/LS) at mild alkaline pH is not substantially affected by forming the complexes. Under certain conditions, isolated CCP(III) exhibits slowly reversible photoreduction, which is predicated on conformational changes in the heme pocket induced by pH (>8.0) (Wang et al., 1992c) or specific mutation of Asp-235 (Wang et al., 1990b, 1993). Figure 10 demonstrates that, while photoreduction still occurs in the complex, it has a reduced yield. However, the kinetics of reoxidation of the photoreduced heme (Figure 11) appear to be unaffected by complexation. It has been suggested (Wang et al., 1992c) that the modulation of the back-transfer

rate (via pH or mutation-induced conformational changes) is responsible for the accumulation of the photoreduced species during laser excitation. The equivalence of the reoxidation rates for the mixture and complex argues that the reduced level of photoreduction in the complexes possibly results from a lower population of the "high-pH" species and not from intrinsically different photodynamic pathways.

SUMMARY/CONCLUSIONS

The data obtained in this study corroborate existing crystallographic (Pelletier & Kraut, 1992) and fluorescence (Anni et al., 1994) results, indicating that CCP/Cytc complexation produces no observable structural alterations in the heme environment of either protein at neutral pH. However, the complexation of CCP and Cytc does induce CD spectral changes in the UV region that most likely originate from the protein conformational alterations in accommodating interprotein interactions. Our results for the equilibrium CCP/horse Cytc electrostatic complexes are consistent with related NMR studies (Moench et al., 1992; Yi et al., 1992, 1993, 1994), which also showed a very small complex-induced NMR change occurring for the CCP/horse Cytc complex. In these respects, the RRS, NMR, and crystallographic studies agree and now present a consistent view of the net response of protein structure upon complexation. We also conclude that the binding of Cytc is able to exert more subtle influences on the pH-dependent flexibility of the CCP active site. These results provide a foundation for a more comprehensive examination of the internal dynamics of CCP/Cytc complexes now in progress.

ACKNOWLEDGMENT

We thank Dr. L. Sparks for the helpful discussion.

REFERENCES

Anni, H., & Yonetani, T. (1992) in *Metal Ions in Biological Systems* (Sigel, H., & Sigel, A., Eds.) Vol. 28, pp 219−241, Marcel Dekker, Inc., New York.

Anni, H., Vanderkooi, J. M., Sharp, K. A., Yonetani, T., & Hopkins, S. C. (1994) *Biochemistry 33*, 3475−3486.

Bosshard, H. R., Anni, H., & Yonetani, T. (1991) in *Peroxidases in Chemistry and Biology* (Everse et al., Eds.) Vol. 2, pp 51−83, CRC Press, Boca Raton, FL.

Cartling, B. (1988) in *Biological Applications of Raman Spectroscopy* (Spiro, T. G., Ed.) Vol. 3, pp 217−248, Wiley, New York.

Choudhury, K., Sundaramooethy, M., Hickman, A., Yonetani, T., Woehl, E., Dunn, M. F., & Poulos, T. L. (1994) *J. Biol. Chem. 269*, 20239−20249.

Cokic, P., & Erman, J. E. (1987) *Biochim. Biophys. Acta 913*, 257−271.

Conroy, C. W., Tyma, P., Daum, P., & Erman, J. E. (1978) *Biochim. Biophys. Acta 537*, 619−622.

Dasgupta, S., Rousseau, D. L., Anni, H., & Yonetani, T. (1989) *J. Biol. Chem. 264*, 654−662.

Edwards, S. L., & Poulos, T. L. (1990) *J. Biol. Chem. 265*, 2588−2595.

Erman, J. E., & Vitello, J. B. (1980) *J. Biol. Chem. 255*, 6224−6227.

Erman, J. E., Vitello, L. B., Mauro, J. M., & Kraut, J. (1989) *Biochemistry 28*, 7992−7995.

Evangelista-Kirkup, R., Smulevich, G., & Spiro, T. G. (1986) *Biochemistry 25*, 4420−4425.

Finzel, L. A., Farnum, M. F., Mauro, J. M., Miller, M. A., Kraut, J., Lin, Y., Tan, X., & Scholes, C. P. (1991) *Biochemistry 30*, 1986−1996.

Garber, E. A. E., & Margoliash, E. (1994) *Biochim. Biophys. Acta 1187*, 289−295.

Geren, L., Hahm, S., Durham, B., & Millett, F. (1991) *Biochemistry 30*, 9450−9457.

Goodin, D. B., & McRee, D. E. (1993) *Biochemistry 32*, 3313−3324.

Hahm, S., Durham, B., & Millet, F. (1992) *Biochemistry 31*, 3472−3477.

Hahm, S., Miller, M. A., Geren, L., Kraut, J., Durham, B., & Millet, F. (1994) *Biochemistry 33*, 1473−1480.

Hashimoto, S., Teraoka, J., Inubushi, T., Yonetani, T., & Kitagawa, T. (1986) *J. Biol. Chem. 261*, 11110−11118.

Hildebrandt, P., English, A. M., & Smulevich, G. (1992) *Biochemistry 31*, 2384−2392.

Hoffman, B. M., Ratner, M. A., & Wallin, S. A. (1990) in *Electron Transfer in Biology and the Solid State* (Johnson, M. K., et al., Eds.) pp 125−146, American Chemical Society, Washington, DC.

Kitagawa, T. (1988) in *Biological Applications of Raman Spectroscopy* (Spiro, T. G., Ed.) Vol. 3, pp 97−131, Wiley, New York.

Leonard, J. J., & Yonetani, T. (1974) *Biochemistry 13*, 1465−1468.

Liu, R.-Q., Hahm, S., Miller, M. A., Durham, B., & Millett, F. (1995) *Biochemistry 34*, 973−983.

Margoliash, E., & Frohwirt, N. (1959) *Biochem. J. 71*, 570−572.

Mauk, M. R., Ferrer, J. C., & Mauk, G. A. (1994) *Biochemistry 33*, 12609−12614.

Mauro, J. M., Fishel, L. A., Hazzard, J. T., Meyer, T. E., Tollin, G., Cusanovich, M. A., & Kraut, J. (1988) *Biochemistry 27*, 6243−6256.

Mauro, J. M., Miller, M. A., Edwards, S. L., Wang, J., Fishel, L. A., & Kraut, J. (1989) in *Metal Ions in Biological Systems* (Sigel, H., & Sigel, A., Eds.) Vol. 25, pp 477−503, Marcel Dekker Inc., New York.

McLendon, G. (1988) *Acc. Chem. Res. 21*, 160−167.

McLendon, G. (1991) in *Metal Ions in Biological Systems* (Sigel, H., & Sigel, A., Eds.) Vol. 27, pp 183−198, Marcel Dekker Inc., New York.

Miller, M. A., Hazzard, J. T., Mauro, J. M., Edwards, S. L., Simons, P. C., Tollin, G., & Kraut, J. (1988) *Biochemistry 27*, 9081−9088.

Miller, M. A., Liu, R.-Q., Hahm, S., Geren, L., Hibdon, S., Kraut, J., Durham, B., & Millett, F. (1994a) *Biochemistry 33*, 8686−8693.

Miller, M. A., Han, G. W., & Kraut, J. (1994b) *Proc. Natl. Acad. Sci. U.S.A. 91*, 11118−11122.

Moench, S. J. (1986) Ph.D. Dissertation, Colorado State University.

Moench, S. J., Satterlee, J. D., & Erman, J. E. (1987) *Biochemistry 26*, 3821−3826.

Moench, S. J., Chroni, S., Lou, B., Erman, J. E., & Satterlee, J. D. (1992) *Biochemistry 31*, 3661−3670.

Myer, Y. P. (1985) *Curr. Top. Bioenerg. 14*, 149−188.

Nuevo, M. R., Chu, H.-H., Vitello, L. B., & Erman, J. E. (1993) *J. Am. Chem. Soc. 115*, 5873−5874.

Pellettier, H., & Kraut, J. (1992) *Science 258*, 1748−1755.

Poulos, T. L., & Kraut, J. (1980) *J. Biol. Chem. 255*, 10322−10330.

Poulos, T. L., & Finzel, B. C. (1984) *Pept. Protein Rev. 4*, 115−171.

Ray, G. B., Li, X.-Y., Ibers, J., Sessler, J., & Spiro, T. G. (1994) *J. Am. Chem. Soc. 116*, 162−176.

Rousseau, D. L. (1981) *J. Raman Spectrosc. 10*, 94−99.

Satterlee, J. D., & Erman, J. E. (1984) *J. Am. Chem. Soc. 106*, 1139−1140.

Satterlee, J. D., Moench, S. J., & Erman, J. E. (1987) *Biochim. Biophys. Acta 912*, 87−97.

Shelnutt, J. A., Rousseau, D. L., Dethmers, J. K., & Margoliash, E. (1979) *Proc. Natl. Acad. Sci. U.S.A. 76*, 3856−3859.

Shelnutt, J. A., Satterlee, J. D., & Erman, J. E. (1983) *J. Biol. Chem. 258*, 2168−2173.

Sivaraja, M., Goodin, D. B., Smith, M., & Hoffman, B. M. (1989) *Science 245*, 738−740.

Smulevich, G. (1993) in *Biomolecular Spectroscopy, Part A* (Clark, R. J. H., & Hester, R. E., Eds.) pp 163−193, Wiley, New York.

Smulevich, G., Miller, M. A., Gosztola, D., & Spiro, T. G. (1989) *Biochemistry 28*, 9905−9908.

Smulevich, G., Miller, M. A., Kraut, J., & Spiro, T. G. (1991) *Biochemistry 30*, 9546−9558.
Spiro, T. G. (1988) *Biological Applications of Raman Spectroscopy*, Vol. 3, Wiley, New York.
Spiro, T. G., Smulevich, G., & Su, C. (1990) *Biochemistry 29*, 4497−4508.
Stemp, E. D. A., & Hoffman, B. M. (1993) *Biochemistry 32*, 10848−10865.
Tollin, G., & Hazzard, J. T. (1991) *Arch. Biochem. Biophys. 287*, 1−7.
Wallin, S. A., Stemp, E. D. A., Everest, A. M., Nocek, J. M., Netzel, T. L., & Hoffman, B. M. (1991) *J. Am. Chem. Soc. 113*, 1842−1844.
Wang, J. (1992) Ph.D. Dissertation, University of New Mexico.
Wang, J., Larsen, R. W., Moench, S. J., Satterlee, J. D., & Ondrias, M. R. (1990a) *Biophys. J. 57*, 236.
Wang, J., Mauro, J. M., Edwards, S. L., Oatley, S. J., Fishel, L. A., Ashford, V. A., Xuong, Ng.-h., & Kraut, J. (1990b) *Biochemistry 29*, 7160−7173.
Wang, J., Boldt, N. J., & Ondrias, M. R. (1992a) *Biochemistry 31*, 867−878.
Wang, J., Larsen, R. W., Chan, S. I., Boldt, N. J., & Ondrias, M. R. (1992b) *J. Am. Chem. Soc. 114*, 1487−1488.
Wang, J., Zhu, H., & Ondrias, M. R. (1992c) *Biochemistry 31*, 12847−12854.
Wang, J., Miller, M. A., Zhou, Y., Fan, B., Gao, F., & Ondrias, M. R. (1993) *Biophys. J. 64*, A159.
Wang, J., Rousseau, D. L., Abu-Soud, H. M., & Stuher, D. J. (1994) *Proc. Natl. Acad. Sci. U.S.A. 91*, 10512−10516.
Wang, J., Caughey, W. S., & Rousseau, D. L. (1995a) in *Methods in Nitric Oxide Research* (Feelisch, M., & Stamler, J., Eds.) Wiley (in press).
Wang, J., Takahashi, S., & Rousseau, D. L. (1995b) *Proc. Natl. Acad. Sci. U.S.A.* (in press).
Yi, Q., Erman, J. E., & Satterlee, J. D. (1992) *J. Am. Chem. Soc. 114*, 7907−7909.
Yi, Q., Erman, J. E., & Satterlee, J. D. (1993) *Biochemistry 32*, 10988−10994.
Yi, Q., Erman, J. E., & Satterlee, J. D. (1994) *Biochemistry 33*, 12032−12041.
Yonetani, T., & Ray, G. (1965) *J. Biol. Chem. 240*, 4503−4508.
Zhou, H.-X. (1994) *J. Am. Chem. Soc. 116*, 10362−10375.
Zhou, J. S., & Hoffman, B. M. (1994) *Science 265*, 1693−1696.

BI9518499